First-principles study of magnetoelastic effect in the difluoride compounds MF_{2} (M=Mn, Fe, Co, Ni)

Hena Das, Sudipta Kanungo, and T. Saha-Dasgupta

Phys. Rev. B **86**, 054422 — Published 15 August 2012

DOI: 10.1103/PhysRevB.86.054422

First principles Study of Magnetoelastic Effect in difluoride compounds, MF_2 (M = Mn, Fe, Co, Ni)

Hena Das[1], Sudipta Kanungo[2] and T. Saha-Dasgupta[2]
[1] *School of Applied and Engineering Physics, Cornell University, Ithaca, NY, USA*
[2] *S. N. Bose National Centre for Basic Sciences, Kolkata, India*

Employing first-principle density functional theory (DFT) based calculations, we study the electronic structure and magnetoelastic effect in difluoride compounds MF_2 (M = Mn, Fe, Co, Ni). The magnetoelastic effect driven cell parameter changes across the series are found to exhibit nonmonotonic behavior, in agreement with the recent experimental reports. Our study reveals that this originates from the nonmonotonicity in the exchangestriction of the bond stretching phonon mode associated with the short M-F bond. Our study also uncover the role of M-F covalency in driving the nonmonotonic behavior of M-M exchange interaction across the series.

PACS numbers: 71.15.Mb, 75.80.+q, 63.20.-e

I. INTRODUCTION

The interplay of spin, orbital and lattice degrees of freedom in transition metal oxides (TMO) has been a lively field of study. The general interest in the response of lattice following the changes in magnetism has been revived upon the surge of activity in the field of multiferroics and magnetoelastic effects. While attention has been focused primarily on oxide materials, much less attention has been given to the transition metal fluorides, with F^- ions in the system as opposed to O^{2-} ions. Exploring the fluorides may be a worth while exercise for prediction of new multiferroic or magnetoelastic materials. There have been already theoretical predictions of ferroelectricity in perovskite structured alkaline earth metal fluorides like $NaCaF_3$ or $NaCdF_3$.[1] Based on the symmetry analysis, compounds like $KCrF_4$, $CsCoF_4$ and $KMnFeF_6$ have been predicted[2] to show linear magneto electric coupling, with even possibility of multiferroic behavior. One of the important mechanism which can drive the magnetoelectric behavior is that of magnetostriction, driven by $\sum_{ij} J_{ij}\vec{S}_i.\vec{S}_j$ term in the Hamiltonian. The simplest possible manifestation of the magnetostriction or the static magnetoelastic effect is the change in crystal dimensions responding to the change in magnetism.

Recent neutron powder diffraction experiments[3,4] carried on a series of transition metal difluoride compounds were reported to exhibit interesting magnetostriction effect at the magnetic transition. The compounds investigated include CrF_2, MnF_2, FeF_2, CoF_2, NiF_2, CuF_2.[3,4] Interestingly the involved transition metals in the series are 3d TMs with increasing d occupation of d^4 to d^9. Among this series of compounds CrF_2, CuF_2 are structurally different belonging to distorted monoclinic space group rather than tetragonal structure adopted by the rest.[5] The ordered magnetic structures are also complicated[6] compared to MnF_2, FeF_2, CoF_2, NiF_2, for which a nearly collinear A-type antiferromagnetic (A-AFM) structure is formed below the magnetic ordering temperatures[7]. Leaving aside CrF_2, CuF_2 and considering the high spin state of M cations, as expected for 3d TMF's, the magnetic moment should monotonically decrease from S=$\frac{5}{2}$ for MnF_2 to S=2 for FeF_2 to S=$\frac{3}{2}$ for CoF_2 and S=1 for NiF_2.

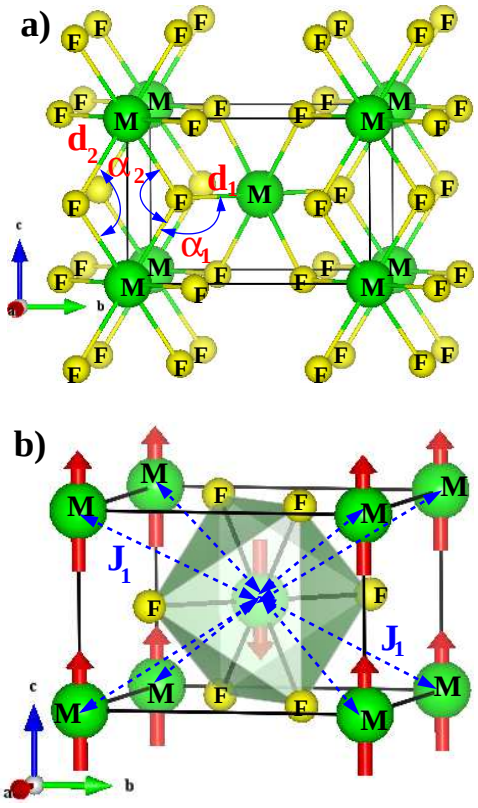

FIG. 1: (Color Online) Crystal (a) and magnetic (b) structure of MF_2. The various important bondlengths and bondangles (see text for details) have been marked in the plot of the crystal structure, while the nearest neighbor magnetic interaction, J_1 has been marked in the plot of the magnetic structure.

The measured magnetovolume effect, however exhibits a rather nonmonotonic trend as a function of magnetic moment with large negative value for the MnF_2, moderately negative values for FeF_2 and NiF_2 and a positive

value for CoF_2 (see Fig. 13 in Ref.6). Although speculations have been made for this curious behavior, to the best of our knowledge, no first principles investigation has been carried out except for the calculation of phonon spectrum for the MnF_2[8] and investigation of covalency effect in FeF_2, NiF_2.[9] In the present study, we carry out a detailed and concise first principle study of MnF_2, FeF_2, CoF_2, NiF_2 which help us in uncovering the origin of this interesting behavior. The present study also establishes the applicability of first principle method in capturing even the tiny magnetoelastic effect correctly, as in the present case.

II. METHODOLOGY

The DFT calculations, reported in the present study, were carried out with choice of three different basis sets, a) plane-wave basis based pseudopotential framework as implemented in the Vienna Abinitio Simulation package (VASP)[10] b) the Linear Muffin Tin Orbital (LMTO) basis[11] and its N-th order extension, NMTO basis[12], as implemented in Stuttgart code[13], and c) the Linear Augmented Plane Wave (LAPW) basis as implemented in WIEN2K code.[14] The consistency of results in three different basis sets have been cross-checked. The exchange correlation function was chosen to be that of generalized gradient approximation (GGA) implemented following the Perdew-Burke-Ernzerhof (PBE) prescription.[14] For the structural optimization, the position of the ions were relaxed towards equilibrium until the Hellman-Feynman forces became less than 0.001 eV/Å. For the plane-wave calculation, a 600 eV plane-wave cutoff was used. A k-point mesh of 6 × 6 × 8 in the Brillouin zone was used for self-consistent calculations. We have also carried out calculations in presence of spin-orbit coupling (SOC), to know its importance in this series of compounds which also provides us with the information of magnetic anisotropic energy. SOC has been included in the calculation in scalar relativistic form as a perturbation to the original Hamiltonian.

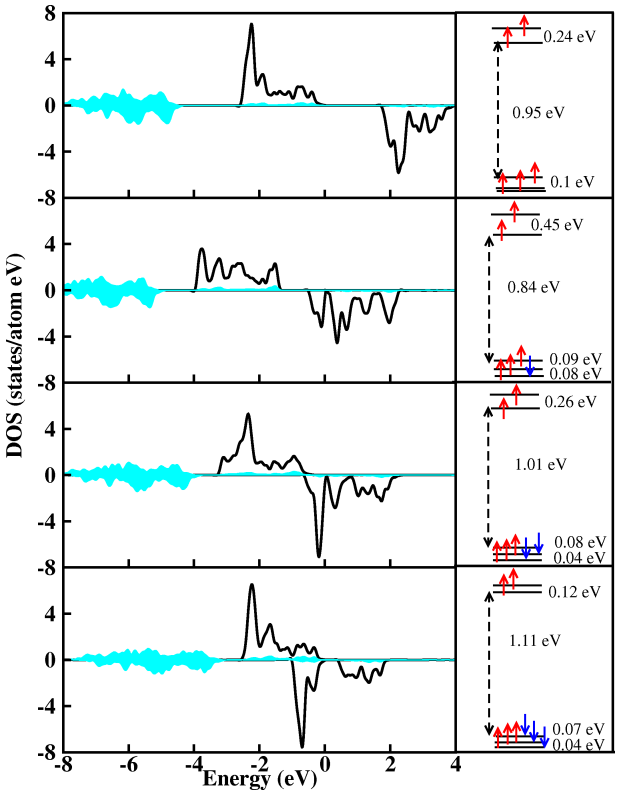

FIG. 2: (Color Online) Left Panels: The spin polarized DOS of MF_2, with M = Mn, Fe, Co and Ni (from top to bottom). The solid, black line and shaded, cyan (grey) area represent DOS projected onto M-d and Fe-p states, respectively. The zero of the energy is set at GGA, Fermi energy. Right panels: The crystal field splitting as well as the occupancies of M-d levels for MF_2, with M = Mn, Fe, Co and Ni (from top to bottom). The lowest two t_{2g} levels for Mn are almost degenerate with tiny separation between them.

III. CRYSTAL AND MAGNETIC STRUCTURE

Transition metal difluorides, MF_2 (M = Mn, Fe, Co, Ni) crystallize in tetragonal rutile type structure of $P4_2/mnm$ space group as shown in the top panel of Fig. 1. The small orthorhombic distortion of NiF_2 below the magnetic transition[9] has been neglected in our study as in the experimental analysis reported in Refs.1,3. The M atoms occupy the high symmetry wyckoff position of 2a while F atom occupy the 4f wyckoff positions with an associated free parameter x. The arrangement of the F^- ions surrounding the M^{2+} site is that of a distorted octahedra, in term of 4 long and 2 short M-F bond lengths and F-M-F bond angles deviating from 90^o. The tetragonal unit cell consist of two formula unit with two M atoms in the unit cell, one at the corner of cell and another at body diagonal position. While two corner MF_6 octahedra are edge sharing along the crystallographic c -direction, through sharing of two F atoms, the MF_6 octahedra at corner and body diagonal position are corner shared through sharing of one F atom. The antiferromagnetic structure given by propagation vector $\vec{k}$= (0,0,1) involves antiparallel alignment of the corner M spins and that at the body centered position, as shown in the bottom panel of Fig. 1. The corner shared M-M antiferromagnetic coupling proceeds through one short M-F bond (d_1), one long M-F bond (d_2) and M-F-M angle of $\approx 130^o$. The edge shared M-M interaction which is of ferromagnetic nature in A-type AFM structure proceeds through equal sized long M-F bonds and M-F-M angles of $\approx 100^o$.

IV. ELECTRONIC STRUCTURE

Fig. 2 shows the spin polarized density of states (DOS) of MF_2 calculated within GGA and projected onto M-d and F-p characters. The distortion of the MF_6 octahedra, lifts the degeneracy of the M-d levels completely in the each of the compounds. The crystal field splitting of metal d levels, together with their occupancies are also shown in Fig. 2. The crystal field splittings were calculated using NMTO-downfolding method,[12] in which M-d states were kept active and the other degrees of freedom were downfolded or integrated out. This leads to the construction of effective, low energy M-d only Hamiltonian. The on-site block of the real-space representation of this low-energy Hamiltonian provides the crystal field splittings. For MnF_2, the majority d levels are completely filled and minority d levels are completely empty, giving rise to an insulating solution with a large band gap of above 2eV and a total magnetic moment of $5\mu_B$/f.u. For FeF_2 and CoF_2 on the other hand d^6 and d^7 occupations of Fe^{2+} and Co^{2+} ions, respectively give rise to partially filled t_{2g} manifold. Nevertheless, the finite splitting between the levels of t_{2g} manifold of the order of 0.08-0.09 eV, gives rise to insulating solution with tiny band gaps even within GGA calculations. The total magnetic moments were obtained as integer values, $4\mu_B$/f.u and $3\mu_B$/f.u for FeF_2 and CoF_2, respectively, in conformity with the insulating solutions. For NiF_2, the large crystal field splitting between t_{2g} and e_g manifolds give rise to a moderate gap value of 1eV with a total magnetic moment $2\mu_B$/f.u and d^8 nominal occupancy of Ni^{2+}. We notice that the F-p dominated DOS is separated from M-d dominated DOS by a gap, the size of which decreases in moving from MnF_2 to FeF_2 to CoF_2 to NiF_2, which in turn increases in the relative hybridization between M-d and F-p degrees of freedom. This is reflected in the computed magnetic moment residing at F site, which turned out to be $0.10\mu_B$, $0.12\mu_B$, $0.13\mu_B$ and $0.15\mu_B$ for the MnF_2, FeF_2, CoF_2 and NiF_2 respectively. We also carried out GGA+SOC calculations, considering the spin quantization axis pointing along the tetragonal c axis [001] and that pointing in ab plane [110]. The [001] orientation of the M spin was found to be favorable in all cases except NiF_2 for which [110] orientation was favored, in good agreement with experimental findings.[16] In conformity with d^5 configuration of Mn, the orbital moment at Mn is found to be tiny, less than $10^{-3}\mu_B$. The partially filled t_{2g} shell of d^6 and d^7 configurations of Fe and Co, gave rise to finite orbital moments, though partially quenched due to lifting of degeneracies within t_{2g} manifold, with values $0.09\mu_B$ and $0.17\mu_B$ respectively. The orbital moment for Co is appreciably high, as has been pointed out in experimental study.[4] Interestingly, we find the orbital moment for Ni to be also rather high, having a value of $0.19\mu_B$. This is unexpected since Ni^{2+} with filled t_{2g} shell and half filled e_g shell, the orbital moment would be quenched. This hints once again to the finite and appreciable hybridization with F-p states as has been concluded in the study of Ref.9. In literature the finite p orbital mixing has been pointed out as a means of generating appreciable SOC effect.[18]

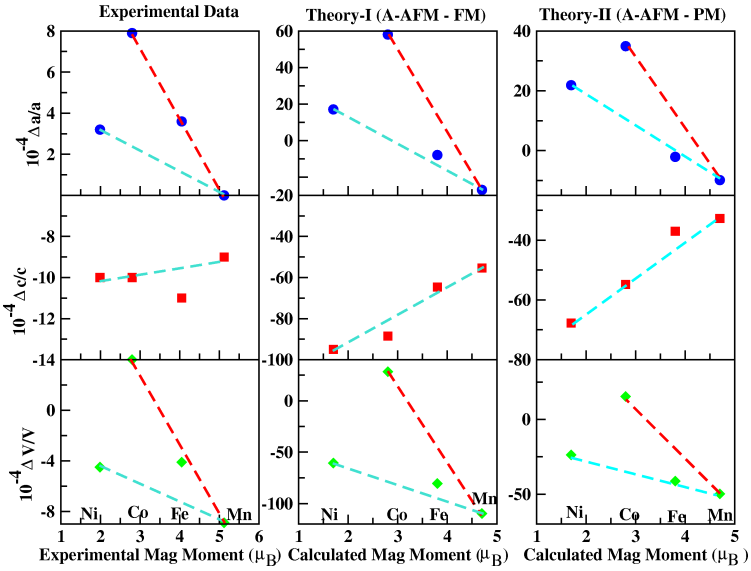

FIG. 3: (Color Online) The relative change in cell parameters, upon change in magnetic ordering for MF_2 (M = Mn, Fe, Co and Ni). The left most panels show the experimental results (extracted out of data points presented in Refs3,4, while the middle and right most panels show the theoretical results (see text for details). Two straight lines have been plotted in the top and bottom panels in order to indicate the non-monotonic behavior of the changes as a function of magnetic moment.

V. MAGNETOELASTIC EFFECT

In the next step, to explore the magnetoelastic effect theoretically, we carried out structural optimization considering the ground state magnetic configurations *i.e* A-AFM and a different magnetic configuration. Ideally, the other magnetic configuration should be the paramagnetic (PM) configuration. However, there is no simple prescription to simulate PM phase in a DFT calculation. We, therefore, consider two different cases. In the first case, the structural changes upon changing the magnetic ordering from FM to A-AFM (*c.f* Theory-I in Fig. 3) were calculated. In the second case, we assumed the PM phase to be mimicked by an average of different possible collinear spin configurations within a supercell of size 2 $\times$ 2 $\times$ 2, which is 8 times the unit cell and containing 16 M atoms in the unit cell. While in principle 2^{16} collinear spin arrangements are possible, among these only six different spin arrangements were chosen which are energetically nondegenrate and compatible with the symmetry of the unit cell. Calculation of structural changes were carried out for all of these six different spin configurations and the average is considered to represent the PM

state (Theory-II in Fig. 3). The results are summarized in Fig. 3, together with experimental results, extracted out of data presented in Refs[3,4]. We find, while $\Delta c/c$ show a more less monotonic behavior within the series MF_2 (M=Mn,Fe,Co,Ni), (with magnetic moment 5,4,3 and $2\mu_B$/f.u) the variation in a lattice parameter ($\Delta a/a$) is highly nonmonotonic. The nonmonotonic behavior of $\Delta a/a$ results into nonmonotonic variation also in volume $\Delta V/V$, which is given by $2(\Delta a/a)+(\Delta c/c)$ for a crystal of tetragonal symmetry. This general trends obtained in theoretical calculations is in very good agreement with experimental measurements. We find $\Delta V/V$ to be relatively large and negative for MnF_2, FeF_2 and NiF_2 being both negative, and that for CoF_2 to be small and positive, in conformity with experimental findings. Considering the quantitative values, theoretical estimates for the first approach (Theory-I) is found to be about a factor 10 larger compared to experimental estimates. Using the supercell approach for defining the PM state (Theory-II) the theoretical estimates are found to be smaller compared to Theory-I, but still a factor 5-6 times larger compared to experimental estimates. Nevertheless, the reduction of values between Theory-II and Theory-I indicates that mimicking the PM state correctly would have presumably made the qualitative comparison between theory and experiment even better. The result presented in Fig. 3 have been obtained with the choice of GGA exchange correlation. We find that introduction of missing correlation effect beyond GGA, in the form of GGA+U calculations,[19] reduce the quantitative estimates even further. However, in absence of good prescription on knowledge of variation of U across the Mn-Fe-Co-Ni series, we have sticked to the result obtained within GGA calculation. One needs to note that such effects are very tiny effects (less than 0.1 %) and therefore it is a challenge both experimentally and theoretically to capture them properly. Keeping that in mind, the overall agreement is surprisingly well.

VI. ORIGIN OF NONMONOTONIC MAGNETOELASTIC BEHAVIOR

In order to probe the origin of observed nonmonotonic magnetoelastic behavior among the studied series, we plot in Fig. 4, the change in various structural elements upon change in magnetic ordering. The structural elements considered are (i) α_1, the AFM corner shared M-F-M bond angle, (ii) α_2, the FM edge shared M-F-M bond angle, (iii) d_1, the short M-F bond forming one edge of the AFM, corner shared interactions, and, (iv) d_2, the long M-F bond forming the other edge of the AFM corner shared interaction (c.f marking in Fig. 1 for visual representation) as well M-F bonds of the edge shared M-M interactions. Note that α_2 connects two M ions situated along the c-axis and the variation in α_2 essentially controls the variation in c, together with that in d_2. The α_1, connects two M ions situated half way

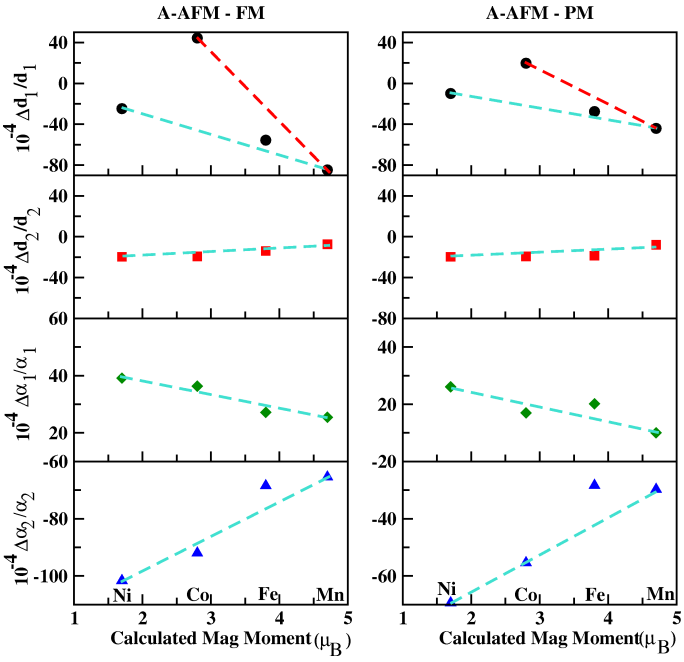

FIG. 4: (Color Online) Calculated changes in structural parameters, d_1, d_2, α_1 and α_2 in MF_2 upon change in magnetic ordering. Two straight lines have been plotted in the top panels, in order to indicate the non-monotonic behavior of the changes as a function of magnetic moment.

through the body diagonal vector and variation is going to effect a, b, c parameters equally. Among the d_1 and d_2 bonds, d_1 bond lie strictly in ab plane while d_2 lies mostly along c axis with relatively smaller component in ab plane. Focusing on the trend of variations of d_1, d_2, α_1 and α_2 as presented in Fig. 4, we find while the variation of the change of d_2 and α_1 (especially d_2) across the series is mild and monotonic, that of α_2 is rather strong and monotonic and that of d_1 is strong and highly nonmonotonic. It is rather interesting to note that the variation of the change α_2 and d_1 almost follows the nature of the variation of the change of "c" and "a" across the series, as presented in Fig. 3. While the exact values of $\Delta a/a$ is determined by variation of both $\Delta\alpha_1/\alpha_1$ and $\Delta d_1/d_1$ (variation of $\Delta d_2/d_2$ being small), the non monotonic behavior of $(\Delta a/a)$ has its origin in the variation in $\Delta d_1/d_1$.

VII. EXCHANGE INTERACTIONS AND PHONONS

The magnetostriction or exchange striction is driven by the spin Hamiltonian $\sum_{ij} J\vec{S}_i.\vec{S}_j$. The superexchange coupling J, depends on (a) the $\angle$ M-F-M, which is α_1 considering the nearest neighbor, AFM interaction in the present case, as $\cos^2\alpha_1$ and (b) $t_{pd}^4/(\Delta + U)$, t_{pd} being the hopping integral connecting F-p and M-d, Δ being

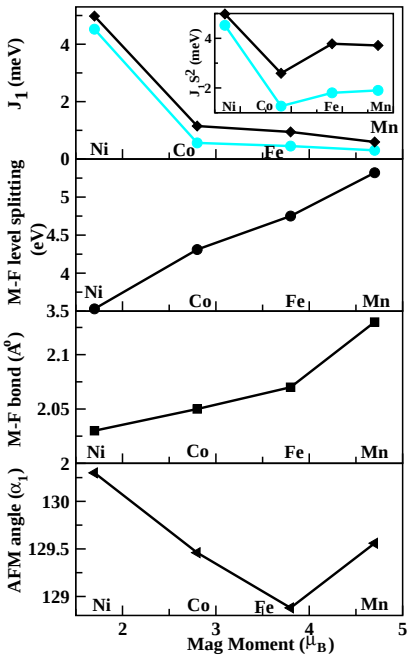

FIG. 5: (Color Online) Top panel: Variation of the magnitude of the nearest neighbor magnetic interaction, J_1 plotted as a function of the magnetic moment, which increases progressively from NiF_2 to CoF_2 to FeF_2 to MnF_2. The inset shows the same for the quantity J_1S^2. The data points marked in cyan (light gray) are from experimental measurements[17] while the points marked in black are theoretical estimates. The rest three panels show the variation of the values of M-F level splitting, M-F bondlength and M-F-M bondangle across the series.

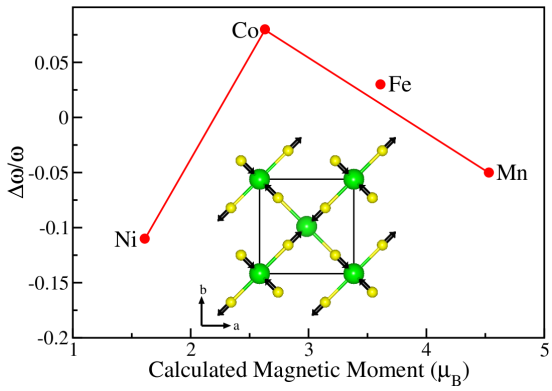

FIG. 6: (Color Online) The relative change in phonon frequency, associated with stretching of short M-F bondlength upon change in magnetic ordering from FM to AFM, for MF_2 compounds, M = Mn, Fe, Co, and Ni. Inset shows the atomic displacements associated with this phonon mode.

the energy level separation between F-p and M-d levels and U being the onsite Coulomb repulsion. t_{pd} depends on M-F bond lengths (d_1, d_2). We extracted AFM NN $J(J_1)$ from total energies of the AFM and FM configurations, calculated within GGA+U with choice of U = 3eV and J_H=0.9 eV and mapping onto a Heisenberg model. The exchange interaction have been also obtained from Neutron inelastic scattering (*c.f* Table IV in Ref.11).[17] The theoretically obtained values of J_1 together with experimental estimates are shown in the top panel of Fig. 5. The chosen values of U and J_H provide good agreement between calculated and measured values of J_1. We find J_1 value for NiF_2 compound is substantially larger compared to the rest in the series, which shows a gradual but small increase in values from MnF_2 to FeF_2 to CoF_2. This results in highly nonmonotonic behavior of J_1S^2 as shown in the inset.

The other three panels of Fig. 5 shows the variation in values of Δ, $\langle d\rangle$ (av. of d_1, d_2) and α_1 across the series. The relatively small Δ, together with small $\langle d\rangle$, which increases t_{pd} value and relatively larger α_1 makes J_1^{Ni-Ni} about a factor of 5 larger compared to that of J_1^{Co-Co}, which over compensates the difference of S^2 between Ni^{2+} and Co^{2+}. J_1S^2 is, therefore, highly nonmonotonic across the series. The change in J_1 value in two magnetic configurations, ΔJ_1, can arise from the change in α_1, $\Delta\alpha_1$ as well as from the change in $\langle d\rangle$, more appropriately in d_1, the change in d_2 being small. While commonly, the magnetostriction giving rise to spin-phonon coupling is associated with the change of superexchange angle upon change in magnetic ordering,[20] we find that in the present case, the metal-anion distance, which dictates the strength of the virtual hopping, t_{pd} also adds on to the exchange striction effect, specially in understanding the non- monotonic behavior of exchangestriction across the series. In order to further probe this issue, we calculate the normal mode frequencies, which are of symmetries, A_{1g}, B_{1g}, A_{2g}, B_{2g}, E_g, B_{1u}, A_{2u} and E_u, for the FM and AFM spin configurations. We calculate the phonon frequencies of the structure optimized with AFM spin configuration. Among the normal modes, the mode A_{1g} is associated with stretching of M-F short bond d_1 (cf inset in Fig. 6). We find while for MnF_2, and NiF_2, phonon frequency associated with A_{1g} mode, softens upon moving from FM to AFM spin alignment, for CoF_2 and FeF_2 ((for FeF_2 the change is small) it is the opposite, phonon frequency hardens in moving from FM to AFM alignment, as shown in Fig. 6. This presumably hints towards the differential behavior of Jahn-Teller nature of the Fe^{2+} and Co^{2+} ions compared to non Jahn-Teller natue of Mn^{2+} and Ni^{2+} ions. We note that Fe^{2+} in its d^6 ($d^5 + d^1$) configuration, has one JT active electron while Co^{2+} in its d^7 ($d^5 + d^2$) configuration has two JT active electrons. This is expected to make the JT influenced changes associated with Co compound to be stronger than that in Fe compound.

VIII. CONCLUSION

In conclusion, using first-principles DFT calculations we have explored the origin of nonmonotonic magnetoelastic effect across the 3-d metal difluoride series MF_2, with M = Mn, Fe, Co and Ni. Our first principles calculations could successfully reproduce the magnetoelastic effect induced nonmonotonic changes in cell parameters for the series as observed experimentally.[3,4] Such an agreement is impressive as the effects are very small. We calculated magnetic exchange interactions as well as investigated magnetic anisotropy effect. Our study indicated the important role of M-F covalency which has been also discussed in literature.[9] The first-principles investigations showed that the nonmonotonic nature of exchangestriction driven changes in lattice across the MF_2 series originates essentially from the nonmonotonic behavior of the bond stretching phonon mode associated with the short M-F bond. While normally attention is paid on the changes in metal- anion-metal super exchange angle, we find that it is the change in metal anion bond that plays the vital role in explaining the nonmonotonic behavior of magnetoelastic effect across the MF_2 series with M = Mn, Fe, Co, Ni.

[1] P. J. Edwardson, L. L. Boyer, R. L. Newman, D. H. Fox, J. R. Hardy, J. W. Flocken, R. A. Guenther and W. Mei, Phys. Rev. B **39**, 9738 (1989); Chun-gang Duan, W. N. Mei1, Jianjun Liu, Wei-Guo Yin, J. R. Hardy, R. W. Smith, M. J. Mehl and L. L. Boyer, Phys. Rev. B **69**, 033102 (2004).

[2] G. Nenert and T. T. M. Palstra, J. Phys.: Condens. Matter. **19**, 406213 (2007).

[3] T. Chatterji, G. N. Iles, B. Ouladdiaf and T. C. Hansen, J. Phys.: Condens. Matter. **22**, 316001 (2010).

[4] T. Chatterji, B. Ouladdiaf and T. C. Hansen, J. Phys.: Condens. Matter. **22**, 096001 (2010).

[5] C. Billy and H. M. Haendler, J. Am. Chem. Soc. **79** 1049 (1957).

[6] T. Chatterji and T. C. Hansen, J. Phys.: Condens. Matter. **23**,276007 (2011).

[7] J. W. Cable, M. K. Wilkinson and E. O. Wollan, Phys. Rev. B **118**, 950 (1960).

[8] R. Schleck, Y. Nahas, R. P. S. M. Lobo, J. Varignon, M. B. Lepetit, C. S. Nelson and R. L. Moreira, Phys. Rev. B **82**, 054412 (2010).

[9] P. J. Brown, B. N. Figgis and P. A. Reynolds, J. Phys.: Condens. Matter. **2**,5297 (1990); *ibid* 5309 (1990).

[10] G. Kresse and J. Hafner, Phys. Rev. B **47**, R558 (1993); G. Kresse and J. Furthmuller, ibid. **54**, 11169 (1996).

[11] O. K. Andersen and O. Jepsen, Phys. Rev. B **12**, 3060 (1975).

[12] O. K. Andersen and T. Saha-Dasgupta, Phys. Rev. B **62**, R16219 (2000).

[13] O. K. Andersen and O. Jepsen, Phys. Rev. Lett. **53**, 2571 (1984).

[14] J. P. Perdew, K. Burke, and M. Ernzerhof, Phys. Rev. Lett. **77**, 3865 (1996).

[15] P. Blaha, K. Schwartz, G. K. H. Madsen, D. Kvasnicka, and J. Luitz, in WIEN2K, An Augmented Plane Wave + Local Orbitals Program for Calculating Crystal Properties, edited by K. Schwarz Technische Universitat Wien, Austria, 2001.

[16] A. Palmes and W. Jauch, Solid State Communication. **77**,95 (1991).

[17] M. T. Hutchings, M. F. Thorpe, R. J. Birgeneau, P. A. Fleury and H. J. Guggenheim, Phys. Rev. B **2**, 1362 (1970).

[18] Chenglong Jia, Shigeki Onoda, Naoto Nagaosa, and Jung Hoon Han, Phys. Rev. B **76**, 144424 (2007).

[19] V. I. Anisimov, I. V. Solovyev and M. A. Korotin, Phys. Rev. B **48**, 16929 (1993).

[20] H. Das, U. V. Waghmare, T. Saha-Dasgupta and D. D. Sarma, Phys. Rev. Lett. **100**, 186402 (2008).